

## **Current control schemes for three-phase four-wire shunt active power filters: a comparative study**

### **Esquemas de control de corriente para un filtro activo trifásico tetrafililar de conexión en paralelo: Estudio comparativo**

*Johann Petit Suárez<sup>1\*</sup>, Hortensia Amarís<sup>2</sup>, Guillermo Robles<sup>2</sup>*

<sup>1</sup>Escuela de Ingenierías Eléctrica, Electrónica y de Telecomunicaciones Universidad Industrial de Santander. Cra 27 calle 9. Bucaramanga – Colombia

<sup>2</sup>Departamento de Ingeniería Eléctrica, Universidad Carlos III de Madrid. Av. Universidad, 30. 28911, Leganés, Madrid-España

(Recibido el 28 de marzo de 2009. Aceptado el 23 de septiembre de 2009)

#### **Abstract**

This paper discusses the performance of different current control schemes used in three-phase four-wire shunt active power filters (APF). The control schemes are based on: Delta Modulation (DM), dead-beat control and PI regulator. The feasibility of the three control schemes have been tested with different waveform and the results are compared through the instantaneous error and the root mean square error between the current of the active power filter and its reference. Finally, the best controller is applied in an experimental setup designed for mitigating harmonics generated by a nonlinear load.

----- *Keywords:* VSI Control, active power filter (APF), power quality, harmonic compensation

#### **Resumen**

El artículo estudia diferentes estrategias de control de corriente usadas en un filtro activo trifásico tetrafililar de conexión en paralelo. Los esquemas de control estudiados son los basados en la Modulación Delta, el control *dead-beat* y el regulador PI. La efectividad de los tres esquemas de control es evaluada al utilizar diferentes formas de onda y los resultados son comparados por medio del error instantáneo y de la raíz media cuadrática del error entre la corriente inyectada por el filtro activo y su referencia. Finalmente, el mejor

---

\* Autor de correspondencia: teléfono: + 57 + 7 + 634 40 00 ext 1293, fax: + 57 + 7 + 635 96 22, correo electrónico: jfpetit@uis.edu.co (J. Petit)

controlador es aplicado en un prototipo experimental de filtro activo diseñado para compensar armónicos generados por una carga no lineal.

----- *Palabras clave:* Control de corriente, filtro activo de potencia, calidad de la energía eléctrica, compensación de armónicos

### Introduction

Nowadays, with the wide use of nonlinear loads and electronic equipment in distribution systems, the problem of power quality (PQ) has become increasingly serious. This fact has led to more stringent requirements regarding PQ which include the search for solutions for such problems [1, 2].

In the case of harmonic pollution, the solution can consider the use of passive filters; however these filters have the disadvantage of having a fixed compensation and can generate resonance problems. In this way, the active power filter (APF) appears as the best dynamic solution for harmonic compensation [3, 4]. In concrete, active power filters are devices designed to improve the power quality in distribution networks. In order to reduce the injection of non-sinusoidal load currents, shunt active power filters can be connected in parallel with the nonlinear loads.

that includes a DC link. The VSI is connected to the point of common coupling (PCC) via a leakage inductance or a transformer. The main purpose of an active power filter is to compensate distorted currents, so that only the fundamental frequency component remains in the grid current. As far as control is concerned, two loops can be identified. The first one is used to calculate the current reference and the second one to guarantee that the reference is exactly followed by the active filter. Regarding the first control loop, strategies based on theories of instantaneous power are the most used; examples of these theories are: the pq theory, and the theory of Fryze. An interesting review of this first control loop is available in [3, 5].

With respect to the second control loop, which is the principal topic of this paper, it must guarantee an accurately track of the sudden variations in the current reference. The second control loop is called current control. Regarding this fact, the hysteresis regulator is the most easy to implement, but it has the disadvantage that can generate a high switching frequency with values time-varying. In this way, the Delta Modulation (DM) appears as solution to above problem [3]. In this case, a fixed switching frequency and a hysteresis band with null value are considered. Together to the Delta Modulation, other control strategies such as those based on dead-beat control and PI-regulator are widely implemented [6, 7, 8]. The choice and implementation of the current regulator is one of the more critical issues for the achievement of a satisfactory performance level, for this reason, in this paper, a comparison among the main current controllers is done, and the best one is tested in a shunt active power filter designed for mitigating harmonics generated by a nonlinear load.

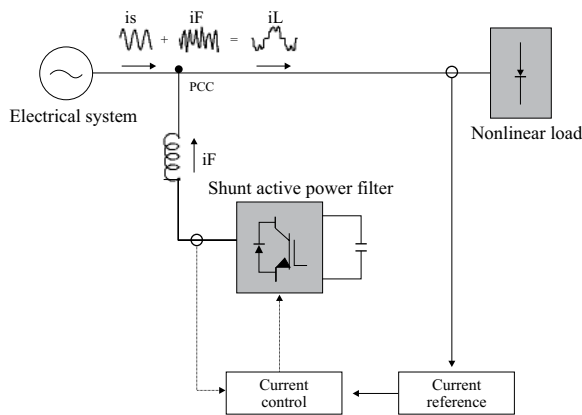


**Figure 1** Shunt active power filter

Figure 1 outlines the main blocks in the electrical circuit for a shunt active power filter. Its main component is a Voltage Source Inverter (VSI)

The organization of the paper is as follows. First, the operation principle of the three control schemes is presented. Then, the comparison among the three current control techniques is discussed. Next the performance of the shunt active filter for mitigating harmonics injected by a nonlinear load is described and finally conclusions are drawn.

## Methodology

### Current Control Schemes

The aim of the controller is to determine the switching actions of the inverter such that the desired current reference is exactly followed. In this paper, the controllers based on Delta Modulation (DM), dead-beat control and PI-regulator are considered. It is assumed that the source is balanced, sinusoidal with frequency  $\omega$ ; the shunt active power filter operates as a controlled voltage source and is connected to the PCC via an inductance that takes into account the leakage inductance of the transformer and the inductance of the filter. A simplified model for a three-phase four-wire shunt active power filter is shown in figure 2.

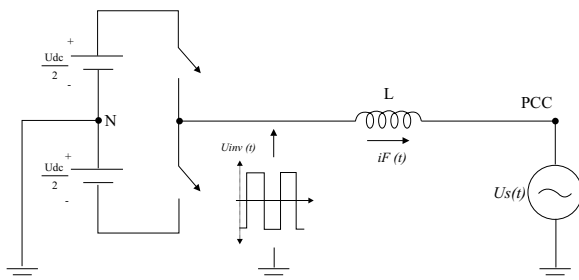


**Figure 2** Single-phase equivalent for a three-phase four-wire shunt active power filter

From this scheme the voltage equation can be written as:

$$L \frac{di_F(t)}{dt} = u_{inv}(t) - u_s(t) \quad (1)$$

Where  $i_F(t)$  represents the generated phase current from the converter;  $u_{inv}(t)$  is the phase-

to-neutral voltage of the inverter and  $u_s(t)$  is the phase-to-neutral voltage of the system.

The current generated at the  $(k+1)$ th sampling time instant,  $i_F(k+1)$ , can be obtained in the discrete form as:

$$i_F(k+1) = i_F(k) + \frac{T_{sw}(u_{inv}(k) - u_s(k))}{L} \quad (2)$$

Where,  $T_{sw}$  is the sampling time. It is considered that the generated phase current ( $i_F$ ), tracks the current reference signal ( $i^*$ ), in the next period as is shown in (3). With regard to the reference signal, it is obtained subtracting the load current to the desired compensated line current.

$$i_F(k+1) = i^*(k+1) \quad (3)$$

From (2) and (3), the active filter control law is obtained as:

$$u_{inv} = \frac{L}{T_{sw}}(i^* - i_F) + u_s \quad (4)$$

### Delta Modulation (DM)

The Delta Modulation method is a variation of the traditional hysteresis current regulator [9]. This method consists in applying a constant voltage in all the switching period. The aim of the control is to obtain the switching signals from the comparison between the current error and a fixed tolerance band (normally this band is close to 0). If the mismatch between the actual and reference current is positive, the inverter voltage output must be positive and if the mismatch is negative, the inverter voltage output must be negative. During a regular interval  $T_{sw}$  synchronized with the switching frequency, the voltage is held constant. Figure 3 shows the basic principle of this control strategy for a single-phase equivalent.

If the Delta Modulation is used, the current generated at the  $(k+1)$ th sampling time instant is given as:

$$i_F(k+1) = i_F(k) + \frac{T_{sw} \left( \pm \frac{U_{dc}}{2} - u_s(k) \right)}{L} \quad (5)$$

Where  $i_F(k)$  is the filter current in time  $k$ ,  $T_{sw}$  is the switching period,  $U_{dc}$  is the DC voltage and  $u_s(k)$  is the phase-to-neutral voltage of the system in time  $k$ .

Figure 4 shows the tracking of the current reference with DM method when the inverter voltage output is positive.

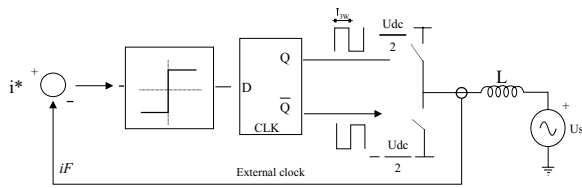


Figure 3 Delta Modulation-basic scheme

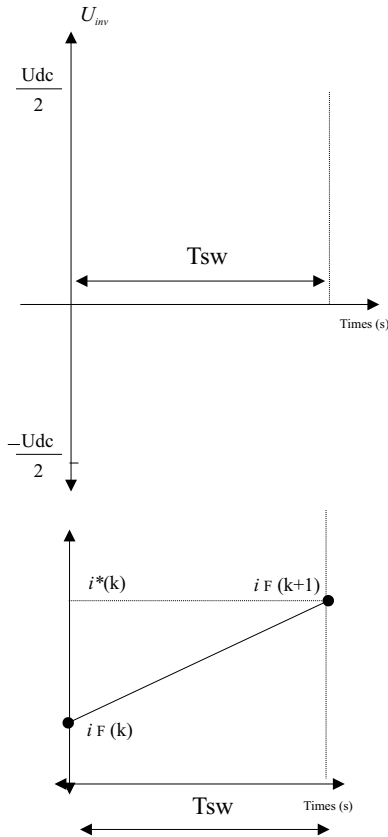


Figure 4 Tracking of the current reference using delta modulation method

### Control method based on dead-beat current control

In the conventional digital dead-beat control schemes, the regulator calculates the phase voltage to make the phase current reach its reference by the end of the following modulation period. In this paper, a modified Method Based on Dead-Beat controller is used (MBDB). The purpose of this method is to compute directly the time period when a switching device is turned on in order to make the phase current reaches its reference by the end of the following modulation period. Figure 5 shows the basic principle of this control strategy for a single-phase equivalent.

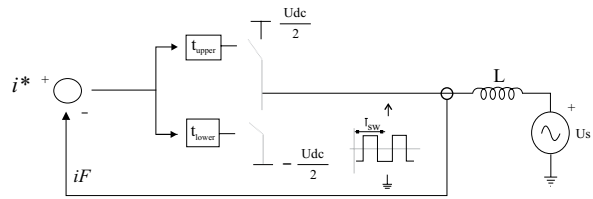


Figure 5 Current regulator based on dead-beat control

The duration of the switching action is calculated considering the average value of the inverter voltage during a sampling interval  $T_{sw}$ . This voltage,  $u_{inv}$ , is based on (4).

$$\bar{u}_{inv} = \frac{L}{T_{sw}} (i^* - i_F) + u_s \quad (6)$$

According to the waveform of figure 6, it can be considered as:

$$\bar{u}_{inv} = \frac{U_{dc}}{2} \left( \frac{2t_{upper}}{T_{sw}} - 1 \right) \quad (7)$$

Where  $t_{upper}$ , represents the time period in which is applied  $\frac{U_{dc}}{2}$  V.

The duration,  $t_{upper}$ , can be obtained from (6) y (7).

$$t_{upper} = \frac{L}{U_{dc}} (i^* - i_F) + \frac{T_{sw}}{2} + \frac{u_s T_{sw}}{U_{dc}} \quad (8)$$

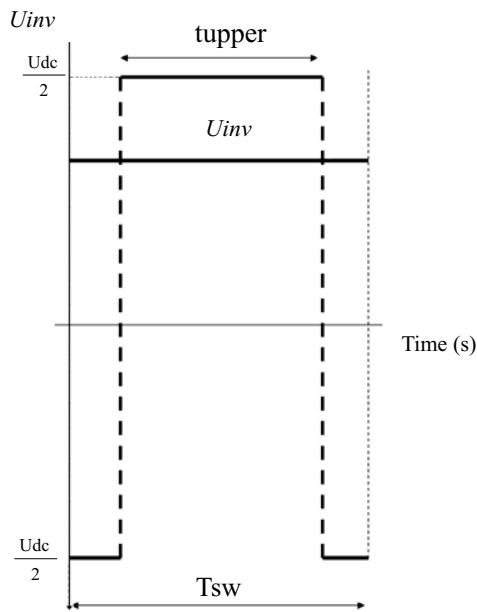


**Figure 6** Voltage waveform in the output of converter using MBDB

In this way, the waveform of current generated is shown in figure 7, and its value at  $(k+1)$ th sampling time instant is given in eq. (9).

$$i_F(k+1) = i_F(k) + \frac{T_{sw}(\bar{u}_{inv}(k) - u_s(k))}{L} \quad (9)$$

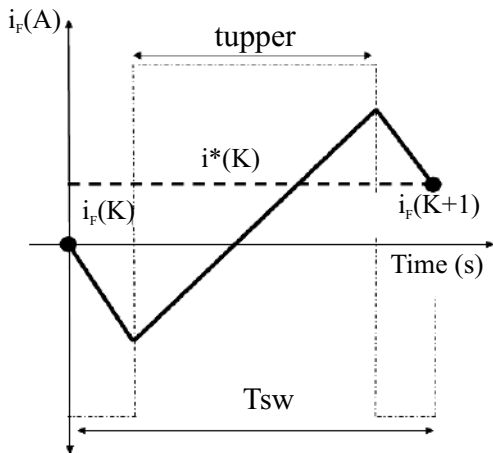


**Figure 7** Tracking of the current reference using MBDB

In this control strategy the number of switches during each sampling interval can be higher than

in the Delta Modulation control. However, when the  $t_{upper} \leq 0$  or  $t_{upper} \geq T_{sw}$ , the control becomes a Delta Modulation.

**PI regulator with triangular carrier (PI)**

This control performs a sine-triangle PWM voltage modulation of the power converter using the current error filtered by a proportional-integral (PI) regulator. In each phase there is a linear PI regulator which compares the current reference and the active filter current, and consequently generates the command voltage. The regulation principle is shown in figure 8.

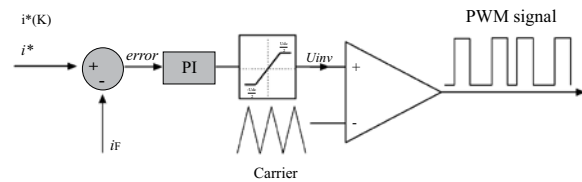


**Figure 8** Current regulator with PI controller

In this case, the time instants at which each switching action is to be performed are evaluated analytically. In this carrier-wave based method (Figure 9), where the switching frequency is equal to the sampling frequency, the command voltage is compared with a triangular wave. If the command voltage is higher than the triangular wave, then upper switching devices are turned on and the lower switching devices are turned off.

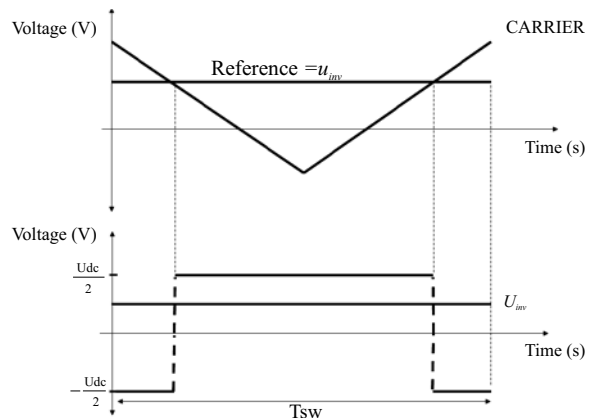


**Figure 9** Voltage waveform in the output of converter using PI control

Due to the uniform sampling, the reference voltage ( $u_{inv}$ ) is constant during the sampling interval,  $T_{sw}$ . The proportional ( $K_p$ ) and integral ( $K_i$ ) parameters of the PI regulator are chosen considering the mathematical model given in (10).

$$u_{inv} = K_p (i^* - i_F) + K_i \int (i^* - i_F) dt \quad (10)$$

The process of adjusting the constants of PI regulator must be accompanied by an analysis of the control system and the results must be verified by means simulations that include the active filter and the power supply. An interesting criterion for adjusting constants can be found in [10, 11].

**Active filter simulation**

The simulations are based on the active filter presented in figure 1. The DC voltage was set to  $U_{dc} = 500$  V, the phase to phase source voltage  $U_L = 230$  V and the inductance,  $L = 20$  mH. In the study, the switching frequency was 10 kHz. However, the methods MBDB and PI involve two commutations by switching period so the switching frequency for the Delta Modulation method was established as 20 kHz. The values used for the PI regulator were adjusted by mean simulations and these are:  $K_p=1$  and  $K_i=0.0006$ .

**Current reference**

The performance of the three current control schemes is compared with different current references: a) Sinusoidal waveform and b) Distorted waveform with a high level of harmonic component. In figure 10 these waveform for a 50 Hz fundamental frequency are shown.

To measure the capability to follow the current reference and evaluate which of the studied methods has a better performance the instantaneous error and the root mean square (RMS) error are considered. Equation (11) shows the instantaneous error between the active filter current and the current reference.

$$\Delta i(t) = i_F(t) - i^*(t) \quad (11)$$

With regard to the root mean square error in a period of the fundamental frequency, this evaluates the ripple in the waveform created by the active filter. However, the quadratic error is not instantaneous; it is averaged in a period of time. This attenuates the effect of peaks in the reference current that would give a large instantaneous error. The equation is shown in (12).

$$\Delta I = \sqrt{\frac{1}{T} \int_0^T (i_F(t) - i^*(t))^2 dt} \quad (12)$$

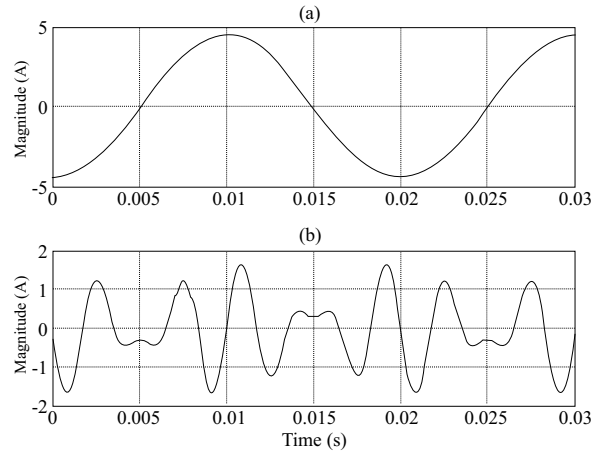


**Figure 10** Current reference, a. Sinusoidal waveform, b. Distorted waveform

The criteria defined in (11) and (12) evaluate the ability of the algorithm to follow the reference and the units are amperes.

**Results**

**Results for a sinusoidal current reference**

In figures 11, 12 and 13, the results for the methods under study are shown. On top are plotted: the phase-to-neutral voltage of the inverter ( $u_{inv}$ ) and the phase-to-neutral voltage of the grid ( $u_s$ ), and on bottom are plotted: the current of the active filter ( $i_F$ ) and its reference ( $i^*$ ).

The methods under study are compared in terms of the instantaneous error and root mean square

error, using a sinusoidal waveform reference. Table 1 shows the figures of merit for this type of waveform and for every method. The root mean square error is calculated in a period of 20ms (50 Hz). The results shown in table 1 confirm that the MBDB method has the best performance.

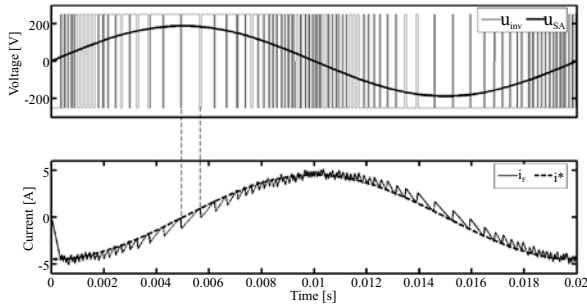


Figure 11 DM Method. Top:  $u_{inv}$  and  $u_s$ . Bottom:  $i_f$  and  $i^*$

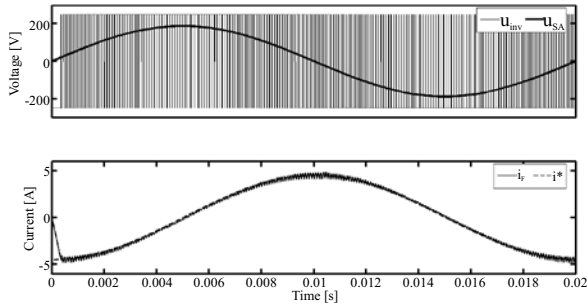


Figure 12 MBDB. Top:  $u_{inv}$  and  $u_s$ . Bottom:  $i_f$  and  $i^*$

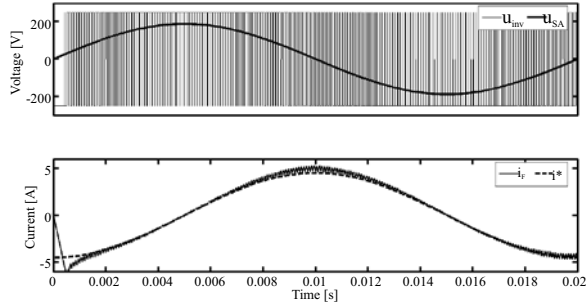


Figure 13 PI Method. Top:  $u_{inv}$  and  $u_s$ . Bottom:  $i_f$  and  $i^*$

**Results for a distorted current reference**

The signal in this simulation is a distorted waveform with a high harmonic content. The

results for this current reference are shown in figures 14, 15 and 16. In this case, the performance of the strategies is really good. The results for the MBDB method are the best. Table 2 shows the results of the criteria of merit for this waveform. Again, it can be concluded that the MBDB method has the best performance.

Table 1 Errors using a sinusoidal waveform reference

	DM (20kHz)	MBDB (10kHz)	PI (10kHz)
$\Delta i_{max}$ [A]	1.148	0.35	0.8
$\Delta$ [A]	0.483	0.168	0.2327

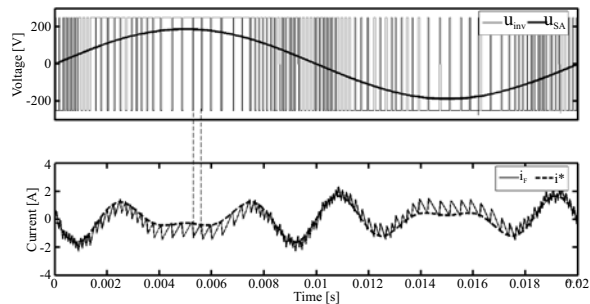


Figure 14 DM Method. Top:  $u_{inv}$  and  $u_s$ . Bottom:  $i_f$  and  $i^*$

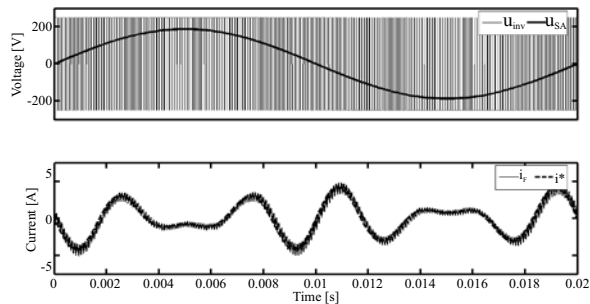
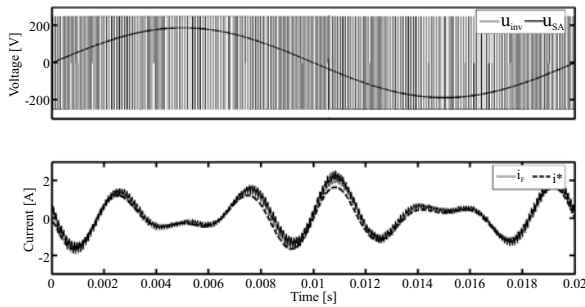


Figure 15 MBDB. Top:  $u_{inv}$  and  $u_s$ . Bottom:  $i_f$  and  $i^*$

Table 2 Errors using a distorted waveform reference

	DM (20kHz)	MBDB (10kHz)	PI (10kHz)
$\Delta i_{max}$ [A]	1.12	0.6207	0.8595
$\Delta$ [A]	0.44	0.2098	0.2601



**Figure 16** PI Method. Top:  $u_{inv}$  and  $u_s$ . Bottom:  $i_f$  and  $j^*$

### Practical application

The results shown above are based on simulations. The feasibility of the hardware implementation for the best current control was evaluated in an experimental setup. This prototype basically included a three phase active power filter, a nonlinear load and a computer with a digital signal processing board, see figure 17.

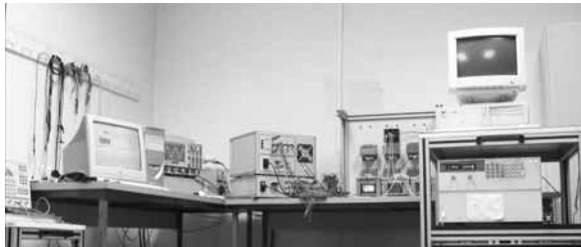


**Figure 17** Photograph of the experimental setup

The power stage consists of a Semikron SKM 50GB 123D inverter with insulated gate bipolar transistor (IGBT) modules. The split capacitors of the DC bus have 2200  $\mu$ F each one and 20 mH branch inductors are applied to suppress the active filter current ripple. In this setup, a d-SPACE 1104 board with a real time computing platform was used to calculate and control the reference current, to communicate the computer running Simulink with the drivers of the IGBTs and to acquire the current and voltage signals. The filter performance was tested with a nonlinear load comprised by a diode rectifier with an AC-side inductor and a resistor and capacitance in the DC-side. The system parameters are summarized in the table 3.

**Table 3** System parameters

$U_L$	$f$	$f_{sw}$	$R$	$L_F$	$U_{dc}$
230V	50Hz	10 kHz	$75\Omega$	20mH	500V

Where,  $f_{sw}$  is the switching frequency,  $R$  is the load resistance of the three phase rectifier,  $f$  is the system frequency,  $L_F$  is the active filter inductance,  $U_{dc}$  is the voltage of the DC bus capacitor and  $U_L$  is the line system voltage.

The waveform to be corrected is the measured current at the input terminals of the load. This is plotted in figure 18 together with the phase-neutral voltage of the grid.

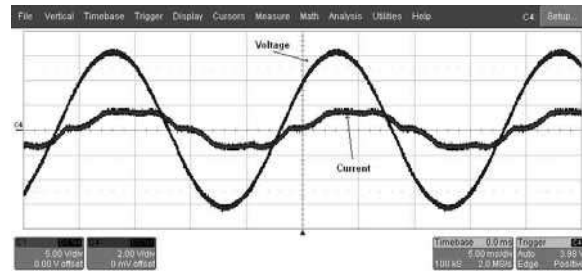


**Figure 18** Voltage signal and grid current before the compensation (phase-a)

The current reference was calculated using the Fryze theory [12, 13] and the current control was implemented with the MBDB method. The results are shown in figure 19. It can be clearly seen that the signal is corrected and a sinusoidal wave substitutes the original waveform when the filter is connected. The results confirm that the MBDB method has an outstanding performance.

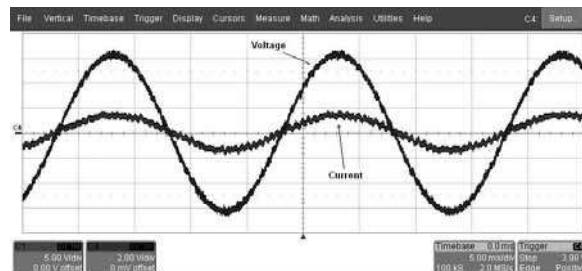


**Figure 19** Voltage signal and grid current after the compensation (phase-a)



## Conclusions

In this paper an active power filter with three different current control methods has been presented and analyzed. The control strategies have been compared, and the results show that the best performance is obtained with the method based on a dead-beat controller. For the sake of simplicity and easy implementation, the method based on Delta Modulation can be utilized. An experimental setup that includes an active power filter and a non-linear load has been analyzed. The results shown the active filter ability for compensating the harmonics generated by the non-linear load, proving the implemented control effectiveness.

## References

1. UNE-EN 61000-3-2. *Límites para las emisiones de corriente armónica (equipos con corriente de entrada  $\leq 16 A$  por fase)*. 2001. pp. 1-29.
2. IEEE std 519. *IEEE Recommended practices and Requirements for harmonic control in electrical power systems*. 1992. pp. 1-100.
3. J. F. Petit. *Control de filtros activos de potencia para la mitigación de armónicos y mejora del factor de potencia en sistemas desequilibrados*. PhD. Thesis. Universidad Carlos III de Madrid. España. 2007. pp. 1-185.
4. B. Singh, K. Al-Haddad, A. Chandra. "A review of active power filters for power quality improvement". *IEEE Trans. Ind. Electron.* Vol. 46. 1999. pp. 960-971.
5. M. Milanés, E. Romero, F. Barrero. "Comparison of Control Strategies for Shunt Active Power Filters in Three-Phase Four-Wire Systems". *IEEE Transactions on Power Electronic.* Vol. 22. 2007. pp. 229-236.
6. S. Buso, L. Malesani, P. Mattavelli. "Comparison of current control techniques for active filter applications". *IEEE Transaction on industrial electronics.* Vol. 45. 1998. pp. 722-729.
7. S. Kumar, P. Agarwal, H. O.Gupta. "A control algorithm for compensation of customer-generated harmonics and reactive power". *IEEE Trans. On Power Delivery.* Vol. 19. 2004. pp. 357-366.
8. Y. Xiaojie, L. Yongdong. "A shunt active power filter using dead-beat current control". *IECON 02, IEEE 2002 28th Annual Conference of the Industrial Electronics Society.* Sevilla (España). Vol. 1. 2002. pp. 633- 637.
9. M. Kazmierkowski, M Dzieniakowski. "Review of current regulation techniques for three-phase PWM inverters". *20th International Conference on Industrial Electronics, Control and Instrumentation. 1994. IECON '94.* Bologna (Italia). Vol. 1. 1994 . pp. 567-575.
10. N. Zargari, G. Joos. "Performance investigation of a current-controlled voltage-regulated PWM rectifier in rotating and stationary frames". *IEEE Trans. Ind. Electron.* Vol. 42. 1995. pp. 396-401.
11. J. F. Petit, H. Amarís, G. Robles. "Control schemes for shunt active filters to mitigate harmonics injected by inverted-fed motors". *Proc. 15th Power Systems Computation Conference-PSCC'05.* Liège (Belgium). 2005. Session 22. Paper 6. pp. 1-7.
12. M. Depenbrock. "The FBD-method, a generally applicable tool for analyzing power relations". *IEEE Trans. Power Delivery.* Vol. 8. 1993. pp. 381-387.
13. S. Fryze. "Wirk-, blind- und scheinleistung in elektrischen stromkreisen mit nicht-sinusoidalen verlauf von strom und spannung". *Journal ETZ.* Vol. 25. 1932. pp. 596-599.